Quarterly Letter Report

Growth of AlN and GaN Bulk Crystals from the Vapor Phase

Supported under Grant # N00014-01-1-0301

Office of the Chief of Naval Research

Report for the period 1/1/01-3/31/01

Z. Sitar, R. Schlesser, H. Shin, E. Arkun, R. F. Davis

North Carolina State University

Department of Materials Science and Engineering

Box 7919

Raleigh, NC 27695

REPORT DOCUMENTATION PAGE

Form Approved
OMB No. 0704-0188

1. AGENCY USE ONLY *(Leave blank)*	2. REPORT DATE	3. REPORT TYPE AND DATES COVERED
	March, 2001	Quarterly: 1/1/01 - 3/31/01

4. TITLE AND SUBTITLE

Growth of Single Crystals and Fabrication of GaN and AlN Wafers

5. FUNDING NUMBERS

CFDA: 12.300
DUNS: 008963233
PR: 00PR03598-00
Act.:00312--0051
CAGE: 0ECY3
EDI: 7129AB

6. AUTHOR(S)

Z. Sitar, R. Schlesser

7. PERFORMING ORGANIZATION NAME(S) AND ADDRESS(ES)

North Carolina State University
Hillsborough Street
Raleigh, NC 27695

8. PERFORMING ORGANIZATION REPORT NUMBER

N00014-00-1-0192

9. SPONSORING/MONITORING AGENCY NAMES(S) AND ADDRESS(ES)

Sponsoring: ONR, Code 312, 800 N. Quincy, Arlington, VA 22217-5660
Monitoring: Administrative Contracting Officer, Regional Office Atlanta
Atlanta Regional Office
100 Alabama Street, Suite 4R15
Atlanta, GA 30303

10. SPONSORING/MONITORING AGENCY REPORT NUMBER

11. SUPPLEMENTARY NOTES

12a. DISTRIBUTION/AVAILABILITY STATEMENT

Approved for Public Release; Distribution Unlimited

12b. DISTRIBUTION CODE

13. ABSTRACT ***(Maximum 200 words)***

Prolonged growth of GaN single crystals resulted in decomposed crystals at high ammonia pressures (>430 Torr). Gas composition analysis using quadrupole mass spectrometry revealed that hydrogen concentration in the gas phase increased with increasing ammonia total pressure above 475 Torr in the absence of Ga source and at above 300 Torr in the presence of Ga source. The enhanced decomposition of GaN at higher pressures can be attributed to the role of H_2 in etching of GaN. Decomposition of GaN in the current study may be attributed to thermodynamic instability and evaporation at low total pressures and decomposition due to hydrogen etching as a result of the decomposition of ammonia at high total pressures. Nitrogen dilution of ammonia reduced the amount of hydrogen generated as a result of ammonia decomposition and alleviated decomposition of GaN crystals. A 2 mm x 1.5mm GaN crystal was grown with minimal decomposition via seeded growth in a 40 sccm NH_3 and 20 sccm N_2 gas mixture.

14. SUBJECT TERMS

GaN, AlN, bulk crystal growth, growth from vapor phase, photoluminescence, optical absorption, Raman, SIMS.

15. NUMBER OF PAGES

26

16. PRICE CODE

17. SECURITY CLASSIFICATION OF REPORT	18. SECURITY CLASSIFICATION OF THIS PAGE	19. SECURITY CLASSIFICATION OF ABSTRACT	20. LIMITATION OF ABSTRACT
UNCLAS	UNCLAS	UNCLAS	SAR

Growth of AlN bulk crystals from the vapor phase

Introduction

The following report summarizes research activities related to the growth of AlN over the past quarter (January–March, 2001). The equipment used for this purpose has been described in previous reports.

After implementing software updates and additional hardware safety interlocks, 24-hour growth runs were routinely performed during the past quarter. We focused mainly on the long-term growth at elevated temperatures from AlN source material; both unseeded and seeded growth experiments were conducted and will be discussed below. The following hardware modifications were made to the growth system: (1) parts of the heat insulation of the growth system were replaced and (2) heater connections were re-designed. The new system control window is shown in Figure 1.

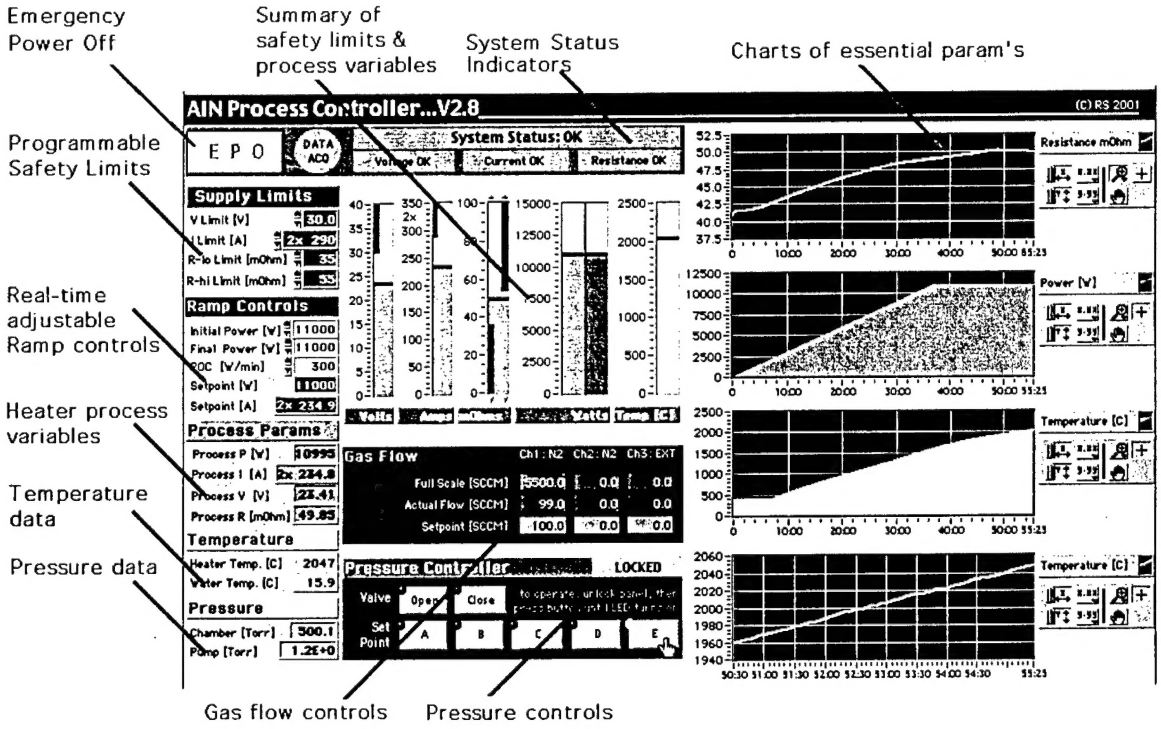

Figure 1: Integrated control window for the AlN growth system.

System hardware

After approximately one year of service, parts of the growth system insulation (porous graphite fiberboard) visibly deteriorated and heat losses from the heater assembly into the external chamber water jacket increased measurably. New insulation material was installed and coated with colloidal graphite paint as an additional protection against surface deterioration. The coated surfaces will be inspected during the following maintenance cycles to evaluate the potential benefits of this additional coating on the long-term stability of the insulation.

Long-term growth experiments at elevated temperatures led to several heater failures. The problem was identified as a hot spot on the graphite heater connection rods close to the base of the heater and was solved by re-designing the connections to decrease their electrical resistance at that location.

Experimental details

A sequence of 24-hour growth runs was performed to test new software and hardware under unattended growth conditions. Apart from the aforementioned insulation and heater problems, the growth system proved to be stable over prolonged periods of time.

Experiments were conducted using AlN source material which was previously formed in the same reactor from metallic Al heated to 2100°C in 500 Torr of nitrogen. Figure 2 illustrates this process.

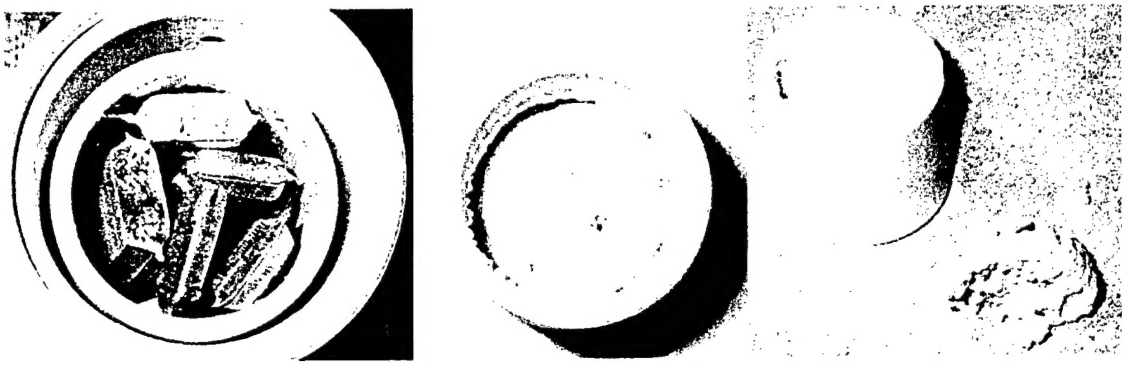

Figure 2: Formation of AlN source material. Metallic Al as loaded into the crucible (left), polycrystalline AlN formed after 2hrs @ 2100°C in 500 Torr N_2 in the crucible (center) and removed from the crucible (right).

After formation of AlN material, the AlN source was installed in a growth crucible and AlN crystals were grown by sublimation for 24 hours at temperatures between 2200 – 2290°C.

Experimental results

Growth parameters were slightly varied to optimize the growth rate. Initial experiments were carried out at temperatures around 2200°C in 500 Torr of nitrogen pressure. Some spontaneous nucleation and growth of AlN single crystals were observed, however, the growth rates were too slow to obtain any sizable crystals within 24 hours.

In order to increase the growth rate, the Al vapor pressure had to be increased in the growth crucible. For this reason, the heater temperature was increased in steps of 20°C per growth run. At above 2250°C, growth rates of 0.5 mm/hr were achieved in the c-direction. Nitrogen pressure was varied as well; some increase in growth rate was observed with decreasing nitrogen pressure. However, as BN becomes unstable at elevated temperatures and at low nitrogen vapor pressures, we used a minimum of 400 Torr nitrogen pressure for all long-term growth runs thus far.

Figure 3 shows an AlN single crystal grown at 2260 C from AlN source material, at a nitrogen pressure of 400 Torr.

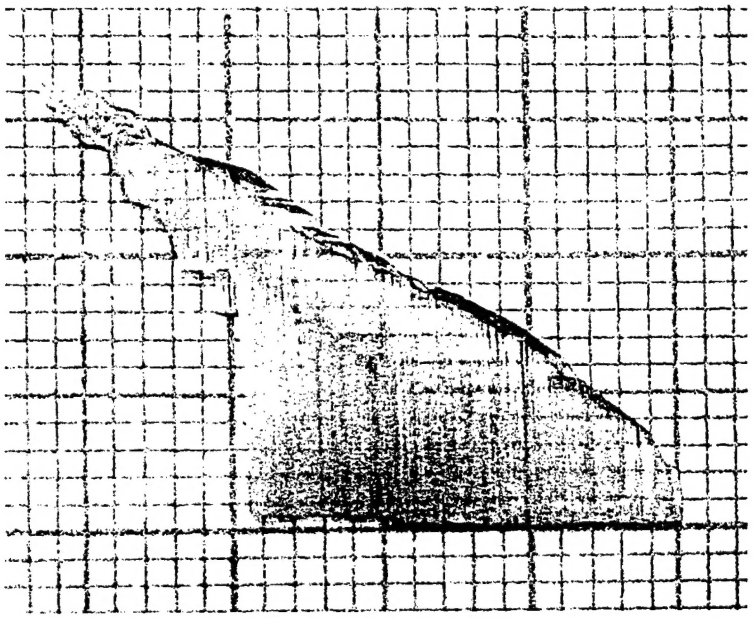

Figure 3: AlN single crystal grown from AlN source material at a temperature of 2260°C and a nitrogen pressure of 400 Torr. Crystallographic c-axis is oriented along vertical surface striations. Line spacing: 1mm. Crystal thickness: 0.5 – 1 mm.

The effective growth rate in c-direction can be estimated from Figure 2, assuming a constant rate over 24 hours. As the crystal grew for (at least) 12 mm in the c-direction, the growth rate was at least 500 μm/hr. The crystal growth was stopped at the crucible wall; the straight edge (Figure 2, bottom) is a consequence thereof. Considering that the crystal might have grown further, the claimed growth rate may be taken as a low estimate.

In all experiments carried out using AlN source material at temperatures above 2200°C, the fastest growth direction was along the c-axis. Growth rates in the c-plane were probably one to two orders of magnitude lower. The striated surface morphology of the crystal shown in Figure 2 is typical for AlN crystals grown under conditions that strongly favor fiber growth in the c-direction.

Conclusion

Long-term growth experiments have shown that growth rates in the c-direction of up to 500 μm/hr can be sustained during prolonged periods of time. Fastest growth occurs along the c-axis, growth in the c-plane is much slower. Even though AlN bulk crystals that grow preferentially in c-direction are ideal for the fabrication of c-oriented wafers, it would be desirable to increase the growth rate in the c-plane to smoothen the striated morphology of these crystals. At this point, we believe that the Al vapor pressure is too low under the above growth conditions. This assumption is supported by the fact that we have been able to grow c-platelets when using metallic Al as a source material, which yields considerably higher Al pressure in the growth crucible.

Decomposition and Growth of Bulk GaN Crystals

Abstract

Prolonged growth of GaN single crystals resulted in decomposed crystals at high ammonia pressures (>430 Torr). Gas composition analysis using quadrupole mass spectrometry revealed that hydrogen concentration in the gas phase increased with increasing ammonia total pressure above 475 Torr in the absence of Ga source and at above 300 Torr in the presence of Ga source. The enhanced decomposition of GaN at higher pressures can be attributed to the role of H_2 in etching of GaN. Decomposition of GaN in the current study may be attributed to thermodynamic instability and evaporation at low total pressures and decomposition due to hydrogen etching as a result of the decomposition of ammonia at high total pressures. Nitrogen dilution of ammonia reduced the amount of hydrogen generated as a result of ammonia decomposition and alleviated decomposition of GaN crystals. A 2 mm x 1.5mm GaN crystal was grown with minimal decomposition via seeded growth in a 40 sccm NH_3 and 20 sccm N_2 gas mixture.

Introduction

Hydrogen release as a byproduct of dissociation of NH_3 may play a significant role in GaN crystal growth. Many researchers have studied decomposition of GaN in the MBE environment. Munir et al. [3] reported that GaN decomposed congruently from a torsion effusion cell when the ratio of the orifice area to sample area was about 0.033 and incongruently when the ratio was 0.01 and less. They measured by a torsion-effusion method the heat of activation for the reaction $2GaN(s) = 2Ga(l) + N_2(g)$ and by a torsion-Langmuir method for the reaction $2GaN(s) = 2Ga(g) + N_2(g)$. Groh et al. [4] found the activation energy of the decomposition of GaN in vacuum to be 3.24 eV in the temperature range from 940°C to 1025°C. Grandjean et al. [5] reported the value of the activation energy to be 3.6 eV in the temperature range between 750–875°C. The observation of a streaky RHEED pattern during the evaporation process was in favor of a layer-by-layer evaporation of the species rather than a crystal decomposition accompanied by degradation of surface morphology. Actually, they did not observe RHEED intensity oscillations during GaN evaporation. This suggests a step-edge evaporation mechanism; if two dimensional evaporation occurs by vacancy formation on terraces one should observe RHEED intensity oscillations by analogy to what is observed when growth proceeds by 2D nucleation. It should be mentioned that the RHEED pattern indicates faceting of the surface when a large amount of material has been evaporated (several thousand angstroms). This could be partly due to an enhanced evaporation rate near defects or/and grain boundaries [6]. Ambacher et al. [7] measured the flux of N_2 and the activation energy of 3.93 eV for GaN decomposition in vacuum by a quadrupole mass spectrometer (QMS). The discrepancy in the activation energy could come from the GaN material used in different experiments. Polarity, surface morphology, crystallinity, crystallographic orientation, and impurities should influence the evaporation rate and thus the activation energy. The high growth temperature and the high vapor pressure of nitrogen led to the problem of nitrogen loss from the GaN film. The loss of nitrogen can be partially alleviated by the use of high V/III gas phase ratios (>2000:1) during the deposition. This is not a problem for the growth of GaN in MBE using atomic nitrogen.

Table I. Decomposition of GaN.

Pressure (Torr)	Temp. (°C)	Gas	Material	Pre-exponent ($cm^{-2}s^{-1}$)	E_A (eV)	Method	Ref.
vacuum	900-1150		Pressed poly-GaN	$4x10^{29}$	3.2	Thermogravimetry	1
vacuum	940-1025		GaN/sapphire	$5x10^{28}$	3.24	Mass spectrometry	2

Averyanova et al. [8] found that there is a critical orifice area at which switching between congruent and incongruent evaporation occurs. Depending on the ratio of orifice area to the

evaporating area of the sample, the gallium vapor pressure in the Knudsen cell can be either higher or lower than the saturated vapor pressure over the liquid gallium. Therefore, incongruent evaporation of GaN is predicted for low orifice area and high temperatures. In contrast, the congruent evaporation should take place at low temperatures and large orifice areas. Munir et al. [3] observed the formation of liquid Ga droplets at the ratio of ~0.01 and no Ga droplets at ~0.033. Averyanova et al. [8] calculated the critical ratio to be $3x10^{-6}$ to $3x10^{-5}$ in the temperature range 890°C~1080°C. The disagreement between the theory and experiment can be due to the uncertainty in evaluation of the sample area in the evaporation experiment. This implies that the decomposition kinetics of GaN can be influenced to a great extent by the ambient gas that affects the concentration of Ga and nitrogen species in the vapor during decomposition.

The influence of ambient gases on the decomposition of GaN has been reported by many researchers [9-17]. They showed that the hydrogen carrier gas had a profound effect on the decomposition. Johnson et al. [9] first reported the decomposition rate of GaN in the stream of H_2 at 800°C to be 0.0016 g/hr. Thurmond and Logan [10, 11] also found that products of the reaction of H_2 with GaN were liquid gallium and ammonia gas in the temperature range from 900°C to 1150°C. A comparison of the NH_3 to H_2 partial pressure ratio at the exit of the reactor revealed a very good agreement with thermodynamic calculations, which means that this reaction is close to equilibrium. Morimoto [12] reported that the decomposition of GaN in H_2 was noticeable at 800°C and liquid Ga was observed at 900°C; no change in weight and surface morphology was observed in N_2 up to 1000°C. Jacob et al. [13] also studied the decomposition of GaN in different gases and found a value of initial decomposition temperature of 970°C in Ar or N_2 and 600°C in H_2. In addition, GaN was not attacked when HCl was mixed with N_2 or Ar, but decomposed when H_2 was added to HCl. Rebey et al. [14] reported that decomposition rate at 1050°C increased rapidly with increasing the H_2 flow rate and reached 30 μm/hr for 3 slm of H_2. They also showed that the increase of N_2 proportion reduced the decomposition rate monotonically, a maximum of 75% reduction being reached for a mixture of 2.5 slm of N_2 and 0.5 slm of H_2. The addition of a small amount of NH_3 to H_2 also inhibited the decomposition of GaN. They have also found the critical temperature of 830°C, at which the rate-limiting decomposition process changed from surface kinetics (E_a ~1.87eV) to diffusion in the boundary layer (E_a~0.38eV). Their interpretation was that the decomposition of GaN started with desorption of surface nitrogen atoms leading to formation of a metallic surface (rich in Ga atoms) having a high reflectivity. Then, the second step of the GaN decomposition was the diffusion of bulk nitrogen atoms towards the surface. When arriving at this surface, the nitrogen atoms were combined to form nitrogen molecules and desorbed. At the same time, there was desorption of Ga species and formation of Ga droplets. Mayumi et al. [15] used an in-situ gravimetric monitoring method to investigate the decomposition of GaN under atmospheric pressure. In the H_2 ambient, the decomposition rate increased exponentially with increasing substrate temperature in the temperature range from 800°C to 950°C. On the other hand, no decomposition of the GaN was observed up to 900°C in He ambient. They also found the decomposition rate of GaN in H_2 and He mixture to be proportional to $P_{H2}^{3/2}$, which indicates that the rate-limiting reaction for the GaN decomposition is

$$GaN(surface) + 3/2H_2(g) = Ga(surface) + NH_3(g)$$

In addition, no Ga droplet was observed on the surface of GaN after the experiment. Thus, the Ga droplets formed by the decomposition of the GaN evaporate immediately with the formation of gaseous GaH_x, which does not play a rate-limiting role in their study. Koleske et al. [16,17] investigated the influence of the H_2 total pressure (10~700Torr) on the decomposition of GaN on sapphire in the temperature range from 850°C to 1050°C. The GaN decomposition rate was accelerated when the H_2 pressure was increased above 100Torr. The mechanism for the enhanced GaN decomposition with increasing pressure is not understood well.

Ga metal is known to dissociate H_2 at high temperatures to form Ga hydrides which may have a higher surface mobility [18]. This was observed by Morishita et al. [19] who demonstrated that Ga diffusion length was increased when H_2 or atomic H were used in the MBE growth of GaAs. They also speculated that GaH_x species were more weakly bound to the surface, and therefore, could diffuse farther before incorporation. The increase in the Ga diffusion length would

more rapidly uncover new areas of the GaN surface for N_2 desorption, which is 10-1000 times faster than the Ga desorption.

Although Ga droplet formation coincides with an increase in the GaN decomposition rate, it is not known if the liquid Ga accumulation is the cause or a result of the increased GaN decomposition rate. The GaN decomposition rate was enhanced at higher pressure (>100Torr) in H_2. This suggests that helps removing N preferentially from the lattice while Ga desorption rate remains relatively constant. When H_2 is replaced by N_2, decomposition rate decreases significantly.

Pisch and Schmid-Fetzer [20] investigated the influence of liquid gallium on the decomposition of GaN in Ar+5%H_2. No significant change in surface morphology was observed for pure GaN samples without liquid gallium at temperatures to 800°C. On the other hand, GaN samples with pre-deposited liquid Ga began to decompose at 720°C. Schoonmaker et al. [21] determined the pressure over GaN and GaN+Ga mixture by weight loss effusion and torsion effusion techniques. The results supported the idea that the vaporization coefficient for the decomposition is much less than unity. In contrast to that, the binary mixture (a direct contact of GaN with liquid Ga) showed considerable dissociation. They proposed that a non-reactant liquid Ga might participate as a catalyst in the vaporization process by dissolving GaN and disrupting its rigid wurtzite crystal structure.

Tanaka and Nakadaira [22] investigated the decomposition of cubic-GaN at various temperatures (800~950°C) in H_2 and estimated the activation energy of 1.6 eV for GaN decomposition. Cubic GaN was annealed in different ambient gases at various temperatures from 800 to 950°C. Cubic GaN remained stable in inert gases but it sublimated in hydrogen ambient. This sublimation was suppressed in H_2 + NH_3 and H_2 + TEG mixtures.

The following sections address decomposition of GaN in ammonia and ammonia-nitrogen mixtures in a bulk GaN growth reactor. The composition of the gas phase was analyzed using mass spectrometry. Based on these results, nitrogen dilution of ammonia was then applied to the growth of GaN bulk crystals to grow larger crystals with minimal decomposition.

Experiment

Gallium nitride thin films used in the decomposition study were grown at 1000°C on SiC substrates with an AlN buffer layer using 26.1 μmol/min of triethylgallium(TEG), 1.5 SLM of NH_3 and 3 SLM of H_2 as a carrier gas at the total pressure of 45 Torr in an MOVPE reactor. GaN thin film, along with several GaN needles of 500μm in length, were placed at the center of the BN susceptor in a dedicated GaN bulk growth reactor for decomposition study. The GaN growth system has been described in detail elsewhere [23]. Processing conditions for decomposition study were the same as those for the growth of bulk GaN crystals except for the absence of the Ga source. The decomposition rates were determined from thickness measurement using scanning electron microscopy (SEM). Surface morphology of the sample after annealing was examined by atomic force microscopy (AFM). Quadrupole mass spectrometry (QMS) was employed to analyze the composition of the gas during heat treatment. An alumina tube of 1/16" inner diameter was used as a sampling probe. The inlet of the tube was placed 3 mm above the BN susceptor, as shown in Figure 1. A differential pumping system was employed between the reactor and the mass spectrometer to maintain the working pressure in the spectrometer chamber below $1x10^{-6}$ Torr. Before each measurement, conditions were allowed to stabilize for 20~30 minutes after any experimental variable was changed. The high temperature nucleation technique [23] used to form the seed crystals consisted of heating the Ga (99.999%) source contained in a BN growth crucible and the susceptor to 1260°C at ~ 20°C/min in nitrogen ambient. At this point, ammonia was introduced in place of nitrogen and susceptor temperature was reduced to commence nucleation. In seeded growth experiments, ammonia was introduced when the BN susceptor temperature reached 1100°C to avoid decomposition of the seed crystals. Grown GaN crystals were subsequently characterized using optical microscopy, scanning electron microscopy(SEM) and x-ray diffraction (XRD). Micro-Raman spectra were obtained at room temperature using a back scattering geometry and 514.5 nm line of an Ar^+ laser. The spot size and the spectral resolution were 4 μm and 1 cm^{-1}, respectively. Photoluminescence (PL) measurements of the samples were made at room temperature using a He-Cd laser (λ=325 nm) as the excitation source. The luminescence detection system

consisted of a 0.5 meter McPherson model 219 scanning vacuum monochromator with a Hamamatsu model R1527-P photomultiplier tube.

Results and Discussion

Figure 2 shows GaN crystals grown at 1130°C and 760 Torr for 2, 8, and 15 hours. The crystal size increased with increasing growth time, however, the crystal surface began to deteriorate after 8 hours of growth and crystals turned white after 15 hours due to surface decomposition.

The decomposition rate of GaN thin films was measured as a function of ammonia pressure and the results are shown in Figure 3. The decomposition rate of GaN decreased as the ammonia total pressure increased from 100 Torr to 510 Torr and increased for higher pressures. A minimum in the decomposition rate of GaN occurred between 430 and 510 Torr at 1130°C. Koleske et al. [24] reported that the minimum decomposition occurred at an ammonia density of $1x10^{19}$ cm^{-3} at 992°C and 150 Torr of NH_3-H_2 total pressure. The higher decomposition rate may be due to a larger concentration of hydrogen in their experiment. One would expect a lower decomposition rate of GaN at higher ammonia pressures. At pressures higher than 510 Torr, however, the decomposition rate increased again. This may be due to a decrease in the suppression of N_2 desorption by NH_3 site blocking due to a gradual increase in the H surface coverage. The increased H coverage may block sites necessary for NH_3 adsorption. Sung et al. [25] determined using time of flight scattering and recoiling spectroscopy (TOF–SARS) that (0001) GaN was terminated by three-fourths of a monolayer of hydrogen bonded to surface nitrogen even without intentional hydrogen exposure and that thermal decomposition with the evolution of H_2 began at 850°C. Unlike NH_3, site blocking with surface H should lead to an increase in the decomposition rate. Reduction in growth rate has been observed at increased total pressures [26] and growth with higher NH_3 fluxes [27]. Growth rate was reduced in H_2 as compared to N_2 carrier gas [7, 28]. The GaN growth rate decreased as the growth pressure increased because of the increased GaN decomposition at higher pressures.

Ammonia decomposes on a GaN surface through the reaction of hydrogen with surface Ga or N depending on the surface termination. Hydrogen can be adsorbed on either Ga sites or N sites, depending on growth conditions, through a surface mediated dissociation of H_2. When H is adsorbed on Ga sites it forms volatile hydrogenated species. The different diffusivity of Ga and N adatoms on GaN surface may provide an explanation for the stability and residence time of N adatoms on the GaN surface. Although N atoms are thermodynamically unstable against desorption as N_2 molecules, the low mobility of this species implies that desorption of N adatoms is kinetically hindered. In order to desorb, the N adatoms have to form molecules. Since the diffusion barrier for N is high (~1.4eV for (0001) and 0.9eV for (000-1) [29, 30], the migration is slow and consequently the residence time of N should be reasonably large. On the other hand, Ga adatoms are very mobile (~0.4eV for (0001) and 0.2 eV for (000-1) [29, 30], the probability that Ga atoms capture N atoms is much higher than the other process where N atoms form molecules and desorb from the surface. Thus, if there are enough Ga atoms present, which is the case under Ga-rich growth conditions, the incorporation probability of N atoms is enhanced. If volatile hydrogenated Ga species are formed, incorporation probability of N atoms into crystal is reduced. Independent of the chemical environment (Ga- or N-rich) polar GaN surfaces turn out to be Ga stabilized. The only known exception so far is an N adatom structure on the (0001) surface found to be stable under very N-rich conditions [31].

Under N-rich growth conditions, the excess N strongly increases the diffusion barrier of Ga adatoms because of the strong bonding of Ga-N. Zywietz et al. [30] found employing density-functional theory calculations that the diffusion barrier of Ga adatoms increased from 0.4 eV to 1.8 eV on (0001) surfaces and from 0.2eV to 1.0 eV on (000-1) surfaces. When hydrogen is adsorbed on GaN surface under N-rich growth conditions, reconstructions maximizing the number of N-H bonds are favored due to the large N-H bond strength. It has been found that hydrogen atoms are bound to the outmost N atoms with a coverage of ~3/4 of a monolayer [32]. Thermal decomposition commenced at ~850°C with the evolution of N_2, NH_2, and H_2, which provides evidence for the existence of N-H bonds on the surface. Surface coverage of H hinders further dissociation of ammonia on the surface and decreases the stability of GaN surface.

It is well known that nitrogen and hydrogen molecules are generated as a byproduct in the reaction of NH_3 with Ga. Nitrogen molecules do not react with Ga or GaN surface because of their strong bonding. Hydrogen, however, is a well-known etchant for GaN. To investigate the cause of the enhanced decomposition at higher pressures than ~510 Torr, the composition of the gas was analyzed by using a quadrupole mass spectrometer. When only NH_3 gas was flowing at a rate of 60 sccm without Ga source in the growth reactor, the hydrogen concentration began to increase at 475 Torr and increased monotonically to 760 Torr. Simultaneously, concentrations of NH_3 and NH_2 began to decrease at 430Torr. The amount of NH_2 in Figure 4 is about 80% of NH_3 concentration, which corresponds well with the ammonia cracking pattern in QMS. The increase in H_2 concentration is attributed to decomposition of NH_3 at 1130°C. Only a trace of hydrogen was detected (<3%) at room temperature. A similar shape of the N_2 curve indicated that hydrogen signal originated from decomposition of ammonia. The reason for the increase in H_2 concentration at ~475 Torr is presently not clear. Figure 4(b) shows the gas composition in the reactor at 1130°C in the presence of Ga. The hydrogen concentration initially began to decrease at 100 Torr and increased abruptly at ~300 Torr. The increase in hydrogen concentration occurred at a lower ammonia pressure (~300Torr) as compared to the case of NH_3 dissociation without Ga. This indicated that more dissociation of NH_3 occurred as a result of the reaction between Ga and NH_3. Ga vapor was not detected in this study due to condensation of Ga on the probe walls on its way to the QMS ionizer. Based on the result of the mass spectrometry, the enhanced decomposition of GaN at higher ammonia pressures is due to an increased hydrogen concentration.

Figure 5 shows AFM images of the GaN surface treated at 1130°C at various ammonia pressures. Treatment at 760 Torr resulted in a very rough surface (~32.6 nm) as a result of enhanced decomposition of GaN. Sample treated at 100 Torr showed a smooth surface (~6.8 nm) despite a higher decomposition rate as shown in Figure 3. Nitrogen desorption rate has been reported to be four orders of magnitude higher than that of Ga at ~1150°C [34]. High decomposition rates obtained at lower ammonia pressures (<300Torr) are more likely due to the thermal instability of GaN than the consequence of chemical reaction with hydrogen.

One way to reduce the hydrogen concentration in the gas phase during the growth is dilution of ammonia with nitrogen. Nitrogen molecules do not dissociate at this growth temperature because of their strong bonding (~9.8eV). Figure 6 shows GaN crystals before and after treatment at 1130°C, at a total pressure of 430 Torr and different nitrogen flow rates. Amber crystals turned to white after treatment in 100% NH_3. When N_2 gas was added to NH_3, the surface became specular as shown in Figure 6(b) and (c). SEM micrographs revealed that free Ga existed on the surface as a result of decomposition. However, the surface of the crystals annealed in 40 sccm NH_3 + 20 sccm N_2 mixture remained smooth even after annealing. Figure 7 shows AFM images of the surface of GaN films after annealing at 1130°C and 430 Torr of total pressure in different gas mixtures. For 60 sccm of pure N_2, GaN film completely decomposed due to a lack of active nitrogen to block the adsorption sites on the surface of GaN. The decomposition rate did not change appreciably for nitrogen dilutions smaller than 20 sccm, as shown in Figure 8. The reason for the minimum decomposition rate at 40sccm NH_3 + 20sccm N_2 is not clear at present.

Kobayashi et al. [35] reported that N desorption from the GaN surface in N_2 carrier gas was suppressed as compared to that in H_2 carrier gas. The activation energy (~1.88 eV) of N desorption in N_2 was larger than that (~0.98 eV) in H_2. They suggested that H_2 carrier gas may react with N atoms on the surface and enhance the N desorption by etching from the GaN surface, whereas the reaction may not occur in the N_2 carrier gas. Figure 9 shows gas composition as a function of nitrogen flow rate. As expected, the hydrogen concentration was higher in the presence of Ga source than in the absence of it.

Based upon the above results, nitrogen dilution of ammonia was applied to seeded growth of bulk GaN crystals. A 2 mm x 1.5 mm GaN crystal was grown at 1130°C and 430 Torr in 36 hrs in a 40 sccm NH_3 + 20 sccm N_2 mixture with minimal decomposition, as shown in Figure 10(a). Well-developed c- and an a-faces of the crystal, showed smooth surface morphology, indicative of suppressed decomposition under the aforementioned growth conditions. XRD patterns taken from c and a faces are shown in Figures 10 (b) and (c), respectively. Without nitrogen dilution, crystals grown under the same growth conditions tended to decompose after ~10hrs of growth and turned into white crystals with very poor surface morphology. Raman spectrum of the crystal grown with

nitrogen dilution showed only the allowed modes of the wurtzite structure, as shown in Figure 11. The excellent crystallinity was confirmed by the FWHM of ~3 cm^{-1} of the Raman $E_2^{(2)}$ mode. A room temperature PL spectrum of the crystal grown in ammonia-nitrogen mixture is shown in Figure 12. Strong bound exciton emission with a FWHM of 85 meV was observed at 365nm (3.4eV). No yellow luminescence was observed in the visible portion of the spectrum.

Conclusion

Prolonged growth of GaN single crystals resulted in decomposed crystals at a high ammonia pressure (~760Torr). Gas composition analysis using quadrupole mass spectroscopy revealed that hydrogen concentration in the gas phase abruptly increased with increasing ammonia pressure at ~300Torr in the presence of Ga which resulted in enhanced decomposition of GaN. Decomposition of GaN in the current study can be attributed to thermodynamic instability and evaporation at low total pressures and decomposition due to hydrogen etching as a result of the decomposition of ammonia at high total pressures. Nitrogen dilution of ammonia reduced the amount of hydrogen generated as a result of ammonia decomposition and increased the kinetic barrier to desorption of reactants from the GaN surface. A 2 mm x 1.5 mm GaN crystal was grown with minimal decomposition via seeded growth in a 40 sccm NH_3 and 20 sccm N_2 mixture.

References

1. Markus Kamp , M. Mayer, A. Pelzmann, K. J. Ebeling, MRS Internet J. Nitride Semicond. Res. **2**, 26 (1997).
2. Esther Kim, I. Berishev, A. Bensaoula, I. Rusakova, K. Waters and J. A. Schultz, J. Appl. Phys., **85**, 1178 (1999).
3. Z. A. Munir, and A. W. Searcy, J. Chem. Phys, **42**, 4223 (1965).
4. R. Groh, G. Gerey, L. Bartha, and J. I. Pankove, Phys. Status. Solidi A **26**, 353 (1974).
5. N. Grandjean, J. Massies, F. Semond, S. Yu. Karpov and R. A. Talalaev, Appl. Phys. Lett., **74** 1854 (1999).
6. S. Guha, N. A. Bojarczuk, and D. W. Kisker, Appl. Phys. Lett., **69,** 2879 (1996).
7. O. Ambacher, M. S. Brandt, R. Dimitrov, T. Metzger, M. Stutzmann, R. A. Fischer, A. Bergmaier and G. Dollinger, J. Vac. Sci. Technol. B **14**, 3532 (1996).
8. M. V. Averyanova, I. N. Przhevalskii, S. Y. Karpov, Y. N. Makarov, M. S. Ramm, R. and A. Talalaev, Mat. Sci. & Eng., B **43**, 167 (1997).
9. W. Johnson, J. Parsons, M. Crew, J. Phys. Chem. **36**, 2651 (1932).
10. C.D. Thurmond, R.A. Logan, J. Electrochem. Soc. **119**, 622 (1972).
11. R.A. Logan, C.D. Thurmond, J. Electrochem. Soc. **119**, 1727 (1972).
12. Y. Morimoto, J. Electrochem. Soc., 1383 (1974).
13. G. Jacob, R. Madar, J. Hallais, Mater. Res. Bull. **11**, 445 (1976).
14. Rebey, T. Boufaden, B. El Jani, J. Crystal Growth, **203**, 12 (1999).
15. M. Mayumi, F. Satoh, Y. Kumagai, K. Takemoto, and A. Koukitu, Jpn. J. Appl. Phys., **39**, L707 (2000).
16. D. D. Koleske, A. E. Wickenden, R. L. Henry, M. E. Twigg, J. C. Culbertson, and R. J. Gorman, Appl. Phys. Lett., **73**, 2018 (1998).
17. D. D. Koleske, A. E. Wickenden, R. L. Henry, M. E. Twigg, J. C. Culbertson, and R. J. Gorman, MRS Internet J. Nitride Semicond. Res. **4S1**, G3.70 (1999).
18. H. Remy, Treatise on Inorganic Chemistry, Elsevier, New York, 18 (1960).
19. Y. Morishita, Y. Nomura, S. Goto, and Y. Katayama, Appl. Phys. Lett., **67**, 2500 (1995).
20. A. Pisch, R. Schmid-Fetzer, J. Crystal Growth **187**, 329 (1998).

21. R. C. Schoonmaker, A. Buhl and J. Lemley, J. Phys. Chem., **69**, 3455 (1965).
22. H. Tanaka, A. Nakadaira, J. Crystal Growth **189/190**, 730 (1998) .
23. H. Shin, D. Thomson, R. Schlesser, Z. Sitar, and R. F. Davis, J. Cryst. Growth, *to be published.*
24. D.D. Koleske, A.E. Wickenden, and R.L. Henry, MRS Internet J. Nitride Semicond. Res. **5S1**, W3.64 (2000).
25. M.M. Sung, J. Ahn, V. Bykov, J.W. Rabalais, D.D. Koleske, and A.E. Wickenden, Phys. Rev. B **54**, 14652 (1996).
26. M.A. Khan, R.A. Skogman, R.G. Schulze, and M. Gershenzon, Appl. Phys. Lett. **43**, 493 (1983).
27. O. Briot, S. Clur, and R.L. Aulombard, Appl. Phys. Lett. **71**, 1990 (1997).
28. M. Hashimoto, H. Amano, N. Sawaki, and I. Akasaki, J. Cryst. Growth, **68**, 163 (1984).
29. T. K. Zywietz, J. Neugebauer, M. Scheffler, J. Northrup and Chris G. Van de Walle, MRS internet J. Nitride Semicon., 3.26 (1998).
30. T. K. Zywietz, J. Neugebauer, M. Scheffler, Appl. Phys. Lett., **73**, 487 (1998).
31. A. R. Smith *et al.*, Phys. Rev. Lett. **79**, 3934 (1997).
32. M.M. Sung, J. Ahn, V. Bykov, J.W. Rabalais, D.D. Koleske, A.E. Wickenden, Phys. Rev. B **54**, 14652 (1996).
33. Cornu and R. Massot, Compilation of Mass Spectral Data, 2nd Ed,
34. D. D. Koleske, A. E. Wickenden, R. L. Henry, W. J. Desisto, and R. J. Gorman, J. Appl. Physics, **84**, 1998 (1998).
35. Y. Kobayashi, N. Kobayashi, J. Cryst. Growth, **189/190**, 301 (1998).

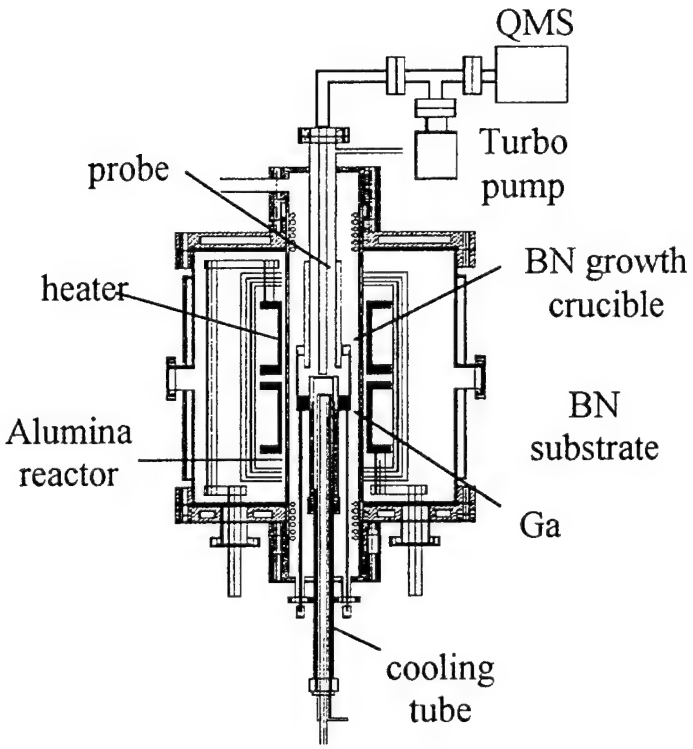

Figure 1. A schematic diagram of the growth chamber with Quadruple mass spectrometer for gas composition analysis.

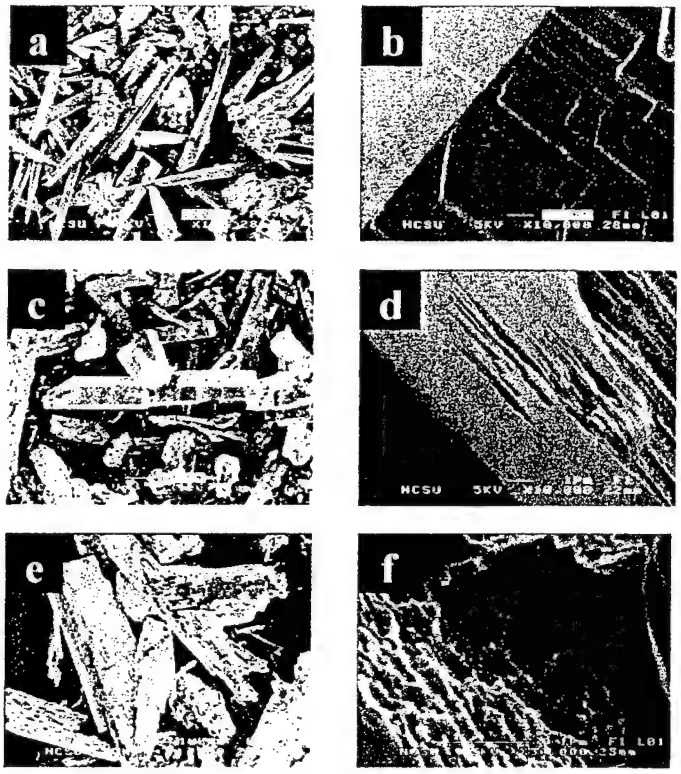

Figure 2. Time-dependent evolution of surface morphology at 1130°C, 760torr of NH_3 for (a) 2hrs, (b) 8hrs,and (c) 15hrs.

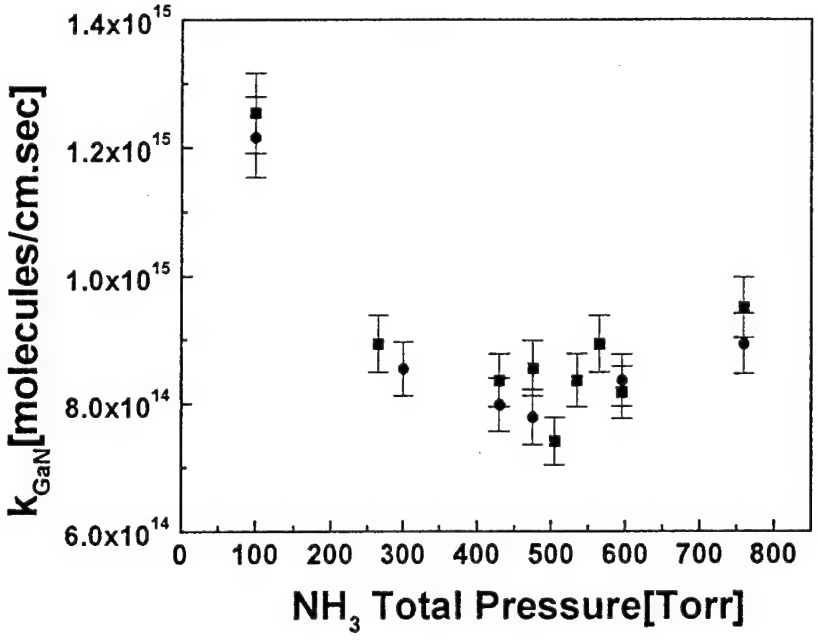

Figure 3. Decomposition rate of GaN at 1130°C, 60sccm of NH_3 in the total pressure range from 100Torr to 760Torr.

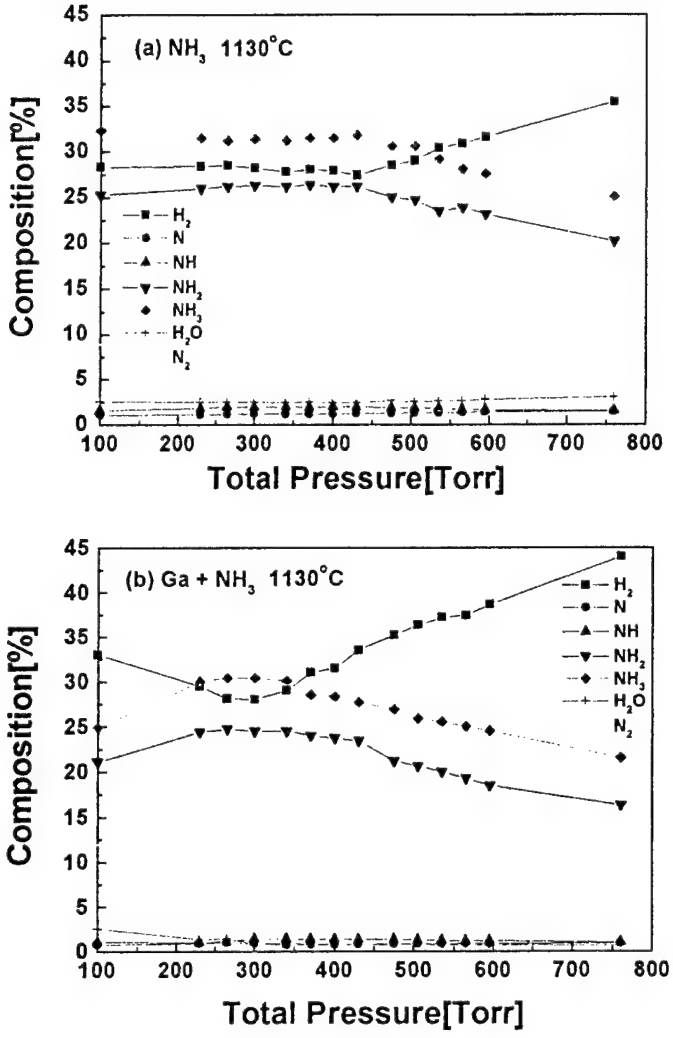

Figure 4. Composition of the gas at 1130°C in the growth reactor (a) with only 60sccm of NH_3 and (b) with NH_3 and Ga.

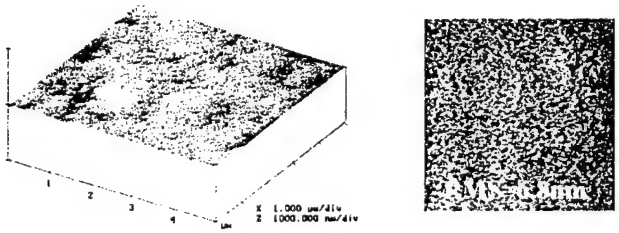

(a)100TorrNH_3

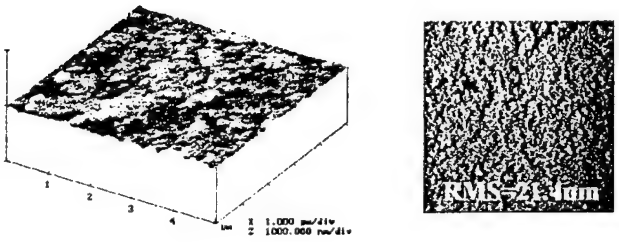

(b)430TorrNH_3

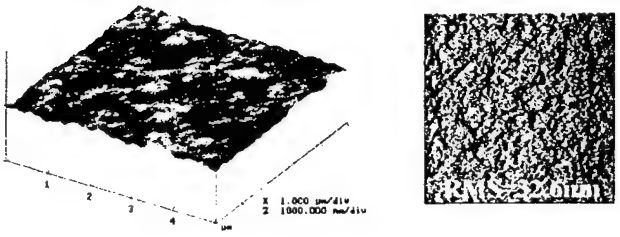

(c)760TorrNH_3

Figure 5. AFM images of GaN samples after annealing at 1130°C, 60sccm of NH_3, and various pressures.

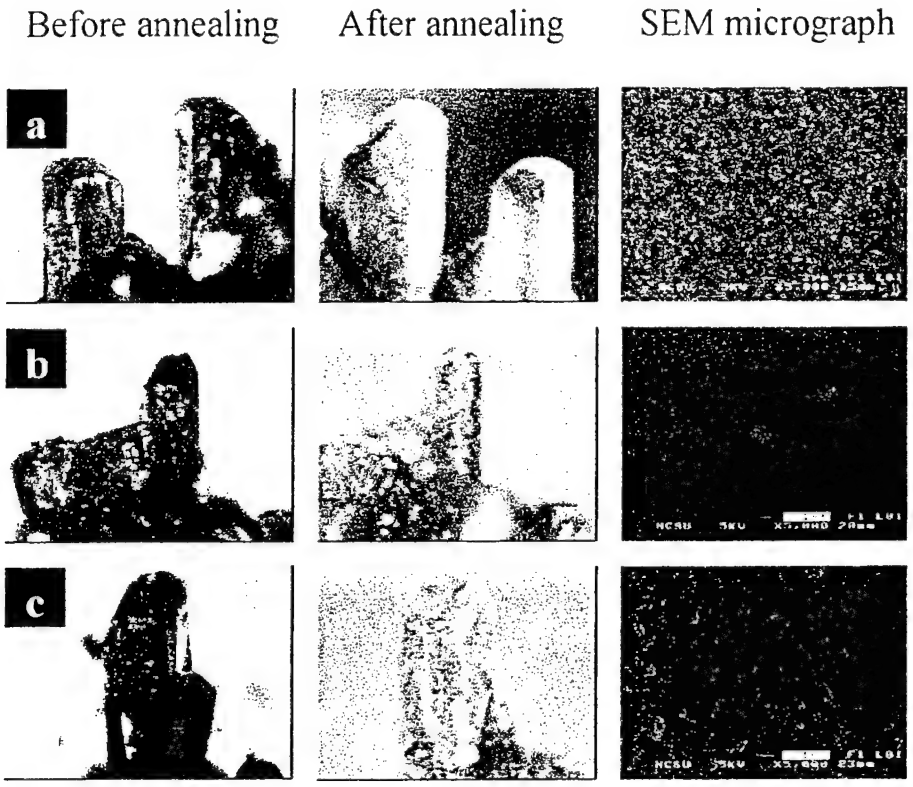

Figure 6. Optical and SEM micrographs of GaN crystals annealed at 1130°C and 430Torr for 2hrs in different ambient gas mixture (a) 60sccm NH_3 (b) 40sccm NH_3 + 20sccm N_2 (c) 20sccm NH_3 + 40sccm N_2

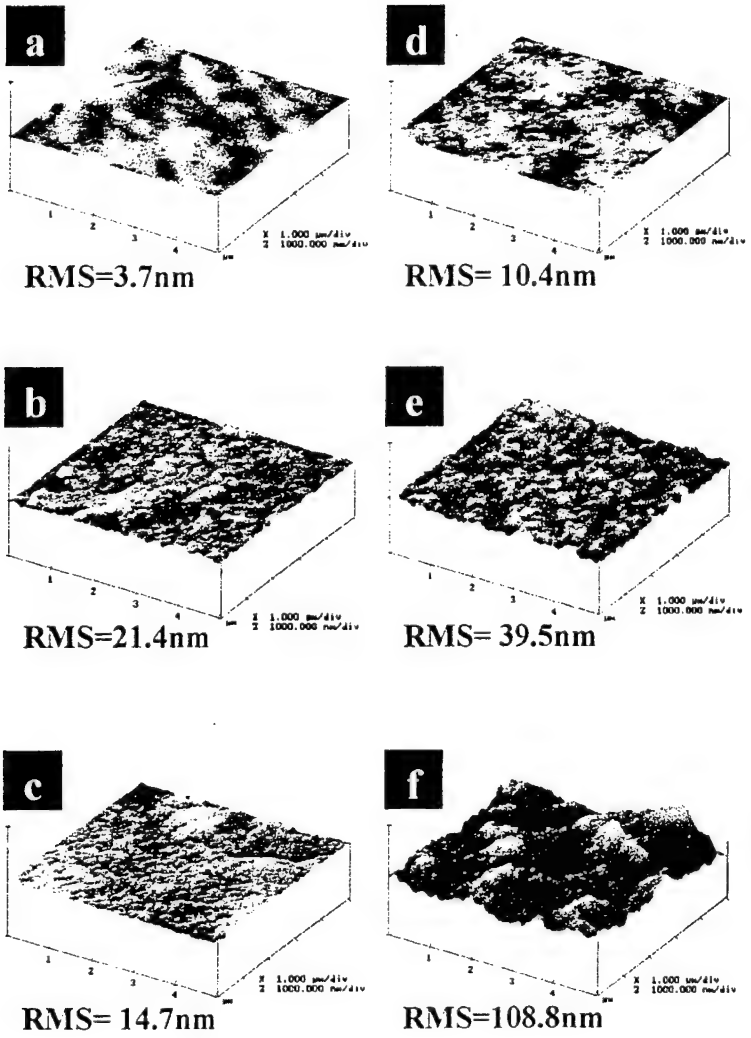

Figure 7. AFM images of GaN samples annealed at 1130°C, 430Torr of different gas mixtures. (a)before annealing, (b)60sccm of NH_3, (c)50sccm NH_3+10sccm N_2, (d)40sccm NH_3+20sccm N_2, (e)30sccm NH_3+30sccm N_2, and (f)20sccm NH_3+40sccm N_2.

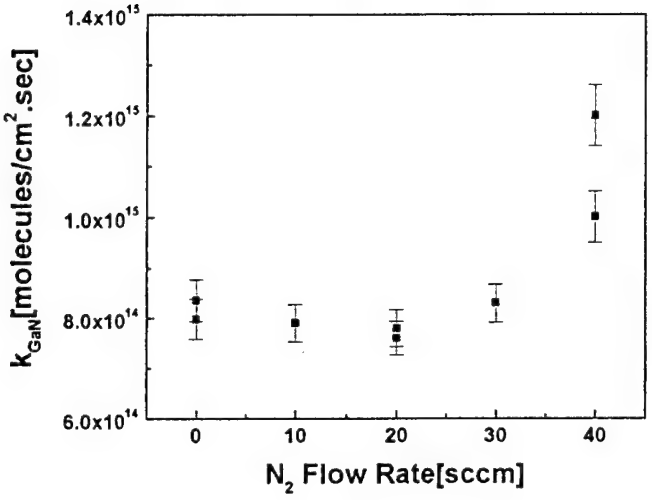

Figure 8. Decomposition rate of GaN at 1130°C, 430Torr in (60-x) sccm NH_3 + x sccm N_2 gas mixture.

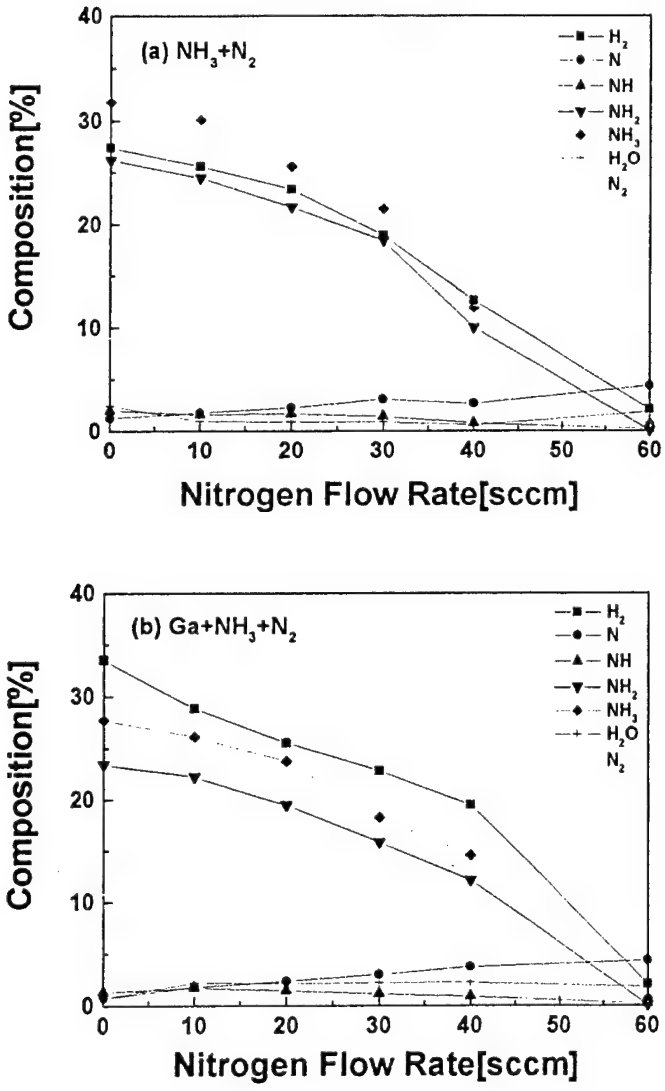

Figure 9. Composition of the gas at 1130°C in the growth reactor (a) without Ga source and (b) with Ga source in (60-x) sccm NH_3 + x sccm N_2 gas mixture.

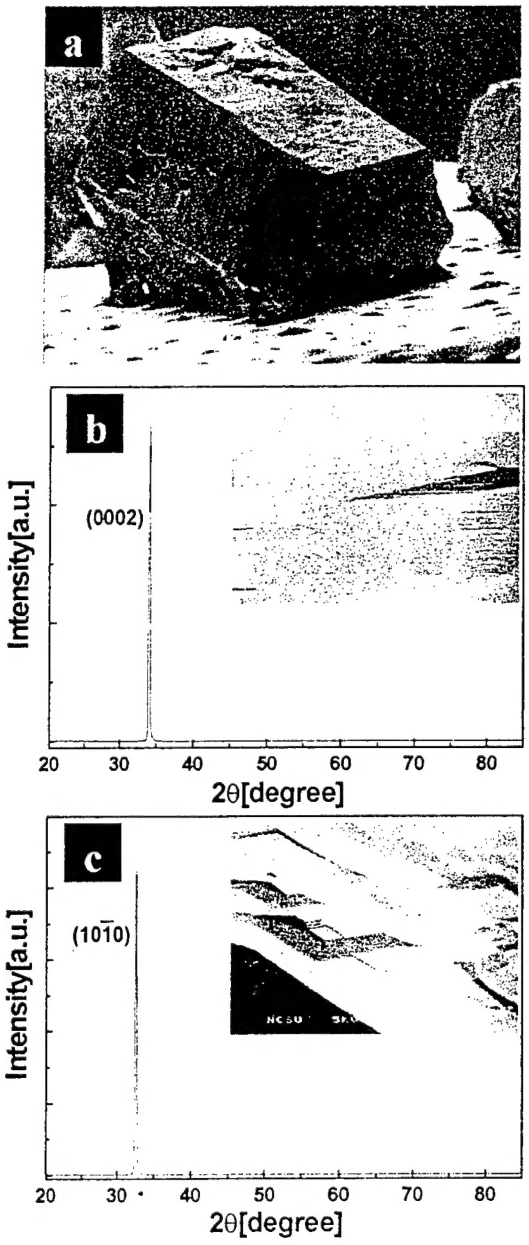

Figure 10. GaN crystal seeded-grown at 1130°C, 430Torr and 40sccm NH_3+20sccm N_2; (a) SEM micrograph (b) XRD pattern and SEM surface morphology of a c-face (c) XRD pattern and SEM surface morphology of a a-face.

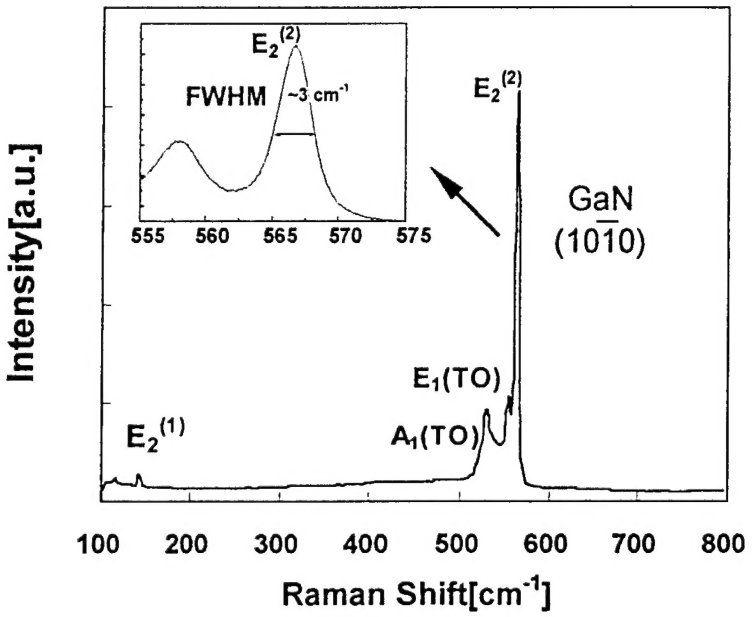

Figure 11. Raman spectrum of the GaN crystal seeded-grown in Fig. 10. Inset is a magnified view of the $E_2^{(2)}$ peak.

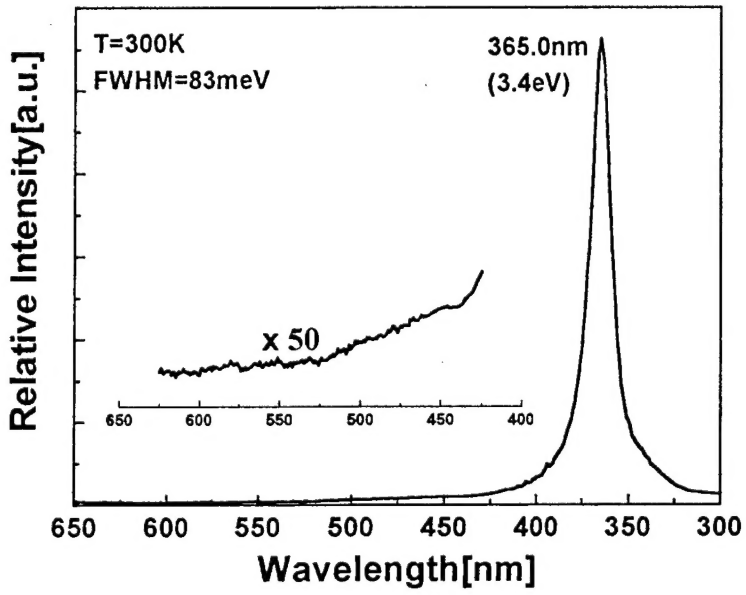

Figure 12. Photoluminescence spectrum of the bulk GaN crystal shown in Fig. 10(a)

Distribution List

Dr. Colin Wood Office of Naval Research Electronics Division, Code: 312 Ballston Tower One 800 N. Quincy Street Arlington, VA 22217-5660	3
Administrative Contracting Officer Office of Naval Research Regional Office Atlanta 100 Alabama Street, Suite 4R15 Atlanta, GA 30303	1
Director, Naval Research Laboratory Attn: Code 2627 Washington, DC 20375	1
Defense Technical Information Center 8725 John J. Kingman Road, Suite 0944 Fort Belvoir, VA 22060-6218	2